Long-range modulation of a composite crystal in a five-dimensional superspace

Laurent Guérin, Céline Mariette, Philippe Rabiller, Michael Huard, Sylvain Ravy, Pierre Fertey, Shane M. Nichols, Bo Wang, Stefan C. B. Mannsfeld, Thomas Weber, Mark D. Hollingsworth, and Bertrand Toudic

Phys. Rev. B **91**, 184101 — Published 5 May 2015

DOI: 10.1103/PhysRevB.91.184101

Long-range modulation of a composite crystal in a five-dimensional superspace

Laurent Guérin,[1] Céline Mariette,[1] Philippe Rabiller,[1] Michael Huard,[1] Sylvain Ravy,[2] Pierre Fertey,[2] Shane M. Nichols,[3] Bo Wang,[3] Stefan C. B. Mannsfeld,[4] Thomas Weber,[5] Mark D. Hollingsworth,[3*] and Bertrand Toudic[1*]

[1]*Institut de Physique de Rennes, UMR UR1-CNRS 6251, Université de Rennes 1, 35042 Rennes, France*

[2]*Synchrotron SOLEIL, L'Orme des merisiers, Saint-Aubin BP 48, 91192 Gif-sur-Yvette cedex, France*

[3]*Department of Chemistry, 213 CBC Building, Kansas State University, Manhattan, Kansas 66506-0401 U.S.A.*

[4]*Center for Advancing Electronics Dresden, Dresden University of Technology, 01062 Dresden, Germany.*

[5]*Laboratory of Crystallography, Eidgenössische Technische Hochschule (ETH) Zurich, CH-8093 Zurich, Switzerland*

*To whom correspondence should be addressed (mdholl@ksu.edu; bertrand.toudic@univ-rennes1.fr)

Abstract

The intergrowth crystal of *n*-tetracosane/urea presents a misfit parameter, defined by the ratio $\gamma = c_h/c_g$ (c_{host}/c_{guest}), that is very close to a commensurate value ($\gamma \cong 1/3$). High-resolution diffraction studies presented here reveal an aperiodic misfit parameter of $\gamma = 0.3369$, which is found to be constant at all temperatures studied. A

complex sequence of structural phases is reported. The high temperature phase (phase I) exists in the four-dimensional superspace group $P6_122(00\gamma)$. At T_{c1} = 179(1) K, a ferroelastic phase transition increases the dimension of the crystallographic superspace. This orthorhombic phase (phase II) is characterized by the five-dimensional (5-D) superspace group $C222_1(00\gamma)(10\delta)$ with a modulation vector $\boldsymbol{a_o}^*+\boldsymbol{c_m}^* = \boldsymbol{a_o}^*+\delta\cdot\boldsymbol{c_h}^*$, in which the supplementary misfit parameter is δ = 0.025(1) in host reciprocal units. This corresponds to the appearance of a modulation of very long period (about 440 ± 16 Å). At T_{c2} = 163.0(5) K, a 5-D to 5-D phase transition leads to the crystallographic superspace group $P2_12_12_1(00\gamma)(00\delta)$ with a very similar value of δ. This phase transition reveals a significant hysteresis effect.

I. INTRODUCTION

The study of aperiodic materials is a rapidly emerging field.[1,2] These materials possess long-range order but no translational symmetry in the physical space of dimension D. All of these materials recover translational symmetry in higher dimensional spaces of dimension (D+d), and they are described within so-called crystallographic superspaces of rank D+d. Aperiodic materials are conventionally divided into three families: quasicrystals,[3,4] incommensurately modulated or magnetic crystals,[5,6] and composite crystals.[7,8] Incommensurately modulated crystals are the simplest of the three because there is always a periodic, high-symmetry phase. The incommensurate phase arises through the appearance of incommensurate modulations, which are described with reference to the mean basic structure of the high symmetry phase. In contrast, incommensurate composite crystals are composed of at least two imbricated subsystems that are incommensurate in at least one direction. The

superspace group of an aperiodic composite is determined by choosing one of the subsystems to define the basis vectors of this modulated subsystem and the vectors of the incommensurate modulations.

In the case of composite aperiodic crystals, supramolecular chemistry and crystal engineering enable very attractive aperiodic host-guest architectures, wherein guest molecules are confined, with their own periodicities, in nanochannels.[9,10] The diffraction patterns of these aperiodic materials exhibit sharp Bragg peaks characteristic of long-range order, although the systems are not invariant under a lattice of translations.[11,12] The crystallographic superspace that describes such materials decomposes into two orthogonal subspaces, the usual physical space and an internal one. For intergrowth nanotubular structures have a single incommensurate direction $\boldsymbol{c}$, a four-dimensional superspace description gives the positions of all of the Bragg peaks[13,15]

$$\boldsymbol{Q}_{hklm} = h\,\boldsymbol{a}^* + k\,\boldsymbol{b}^* + l\,\boldsymbol{c}_h^* + m\,\boldsymbol{c}_g^*, \quad (1)$$

where $\boldsymbol{a}^*$, $\boldsymbol{b}^*$, $\boldsymbol{c}_h^*$ and $\boldsymbol{c}_g^*$ are the conventional reciprocal unit cell vectors, and c_h and c_g refer to the host and the guest parameters. Four indices (h, k, l, and m) are needed to describe the four different types of structure Bragg peaks: a convenient but simplistic labeling is that $h\ k\ 0\ 0$, $h\ k\ l\ 0$, $h\ k\ 0\ m$, and $h\ k\ l\ m$, with l and m different from zero, correspond to the common, host, guest, and satellite Bragg peaks, respectively. However, due to intermodulation, the intensities of the "host" and "guest" Bragg peaks exhibit influences from both substructures.

Urea inclusion compounds constitute a very simple paradigm of self-assembled nanoporous crystals.[15-17] *n*-Alkane/urea (n-C_nH_{2n+2}/($CO(NH_2)_2$)) crystals are typically incommensurate materials, and indeed diffraction patterns with the four types of Bragg

peaks have been reported in these materials.[18-21] Structural instabilities have been extensively studied in these materials.[20-32] High pressure studies demonstrate that the guest-guest interactions along the aperiodic direction can be manipulated,[33] enhancing the interest in further studying the competition between forces in favor of or against commensurability. Here, we focus on *n*-tetracosane/urea (*n*-$C_{24}H_{50}$/urea, Figure 1a,b), an aperiodic composite characterized by a misfit parameter very close to a rational number at ambient conditions: $\gamma = c_h/c_g \cong 1/3$, according to Lenné's formula.[34]

Diffraction studies concerning *n*-alkane/urea inclusion compounds close to commensurability have been reported previously. These include *n*-heptane/urea, where γ is very close to unity (γ = 0.981 at ambient conditions),[21] and *n-h*exadecane/urea, where γ is close to 1/2 (γ = 0.486 at ambient conditions).[20] In *n-h*exadecane/urea, the misfit parameter was found to be constant as a function of temperature at ambient pressure; these composite crystals were therefore aperiodic at all temperatures measured. Only after application of hydrostatic pressure of about 0.40 GPa did this system lock into a commensurate phase with γ = ½.[33] Lock-in was attained by virtue of the larger compressibility along the channel axis of the guest compared to the host, which is extensively hydrogen bonded.

II. EXPERIMENTAL DETAILS

In order to discriminate between large periodicities and incommensurability, measurements were performed using high-resolution laboratory X-rays and very high-resolution synchrotron X-rays. The initial X-ray diffraction measurements were performed using monochromatic Cu-K_α radiation from a rotating anode source and a high-resolution mar345dtb imaging plate detector (Marresearch GmbH), which was

placed as far as 400 mm from the crystal to spatially resolve the Bragg peaks and satellites. Crystals were aligned with their needle axes (**c**) along the phi axis of the goniostat, and rotating crystal measurements were performed. Two types of measurements were conducted: large phi rotations of 60° were used to capture large regions of the accessible diffraction pattern, whereas full data acquisitions with 1º or 2° phi rotation steps were used to reconstruct the required diffraction planes. CrysAlisPro software from Agilent Technologies was used to analyze the full data collections. Local MatLab routines as well as WxDiff[35] were used to analyse individual frames. Diffraction experiments with very high spatial resolution were performed on the CRISTAL beamline at the synchrotron SOLEIL at L'Orme des Merisiers, Gif-sur-Yvette, using an ATLAS CCD detector (Oxford Diffraction) with λ = 1.54980 Å, on beamline 11-3 at the Stanford Synchrotron Radiation Laboratory (SSRL) using a mar345 detector and λ = 0.97440 Å, and on beamline 14-BM-C at the Advanced Photon Source (APS) using an ADSC Quantum 315 CCD detector and a wavelength of λ = 0.97870 Å. Crystals of *n*-tetracosane/urea were grown by slowly cooling a solution of 513 mg of *n*-tetracosane (Aldrich, 99%) and 5.04 g of urea in 23 mL methanol, 48 mL isobutyl alcohol, and 2.2 mL H_2O from 60 ºC to room temperature. ^{1}H Solution NMR spectra (400 MHz, DMF-d_7) showed no detectable amount of either methanol or isobutyl alcohol in the channels.

III. THE HIGH SYMMETRY PHASE (PHASE I) AND THE FERROELASTIC PHASE TRANSITION

Figure 1c shows the 60° oscillation images, obtained on the mar345dtb system, in the high symmetry (HS) phase (Phase I) at room temperature and in the primitive,

low symmetry phase (Phase III) at 100 K. Figure 1b shows the hexagonal and orthorhombic unit cells used for the high and low symmetry phases. In all phases, guest diffraction appears as diffuse layers (which appear as streaks perpendicular to $\boldsymbol{c_g}^*$) with superimposed Bragg peaks. A much more complex signature is revealed at 100 K, as discussed below.

Information concerning the misfit parameters may be extracted by considering the diffraction lines along the reciprocal channel direction. A profile of the $(1\ 0\ l\ m)_h$ layer line (using a hexagonal basis) of Phase I at 200 K generated with synchrotron data from APS 14-BM-C and a detector distance of 980 mm (Figure 2a) shows the clear intermodulation between host and guest and yields a misfit parameter of $\gamma = 0.3369 \pm 0.0005$. At 110 K, the profile of the equivalent $(0\ 2\ l\ m\ n)_o$ layer line (orthorhombic notation) of Phase III (Figure 2b) gives exactly the same misfit parameter of $\gamma = 0.3369 \pm 0.0002$, but with a smaller error due to the larger number of observed peaks, including numerous satellites. Lower resolution studies using the mar345dtb system at thirteen different temperatures confirm the constancy of the misfit parameter from 290 K to 100 K. Using the room temperature unit cell constants for the host ($\boldsymbol{a} = \boldsymbol{b} = 8.20(1)$ Å, $c_h = 11.02(1)$ Å), this yields a value of c_g of 32.71 Å, only slightly shorter than three host repeats (33.06 Å). Thus, although the system is, by construction, exceptionally close to commensurate, and although both host and guest substructures are subject to completely different forces, as illustrated in previous stress-strain measurements,[32,33] no lock-in tendency is observed. *n*-Tetracosane/urea is thus aperiodic at all temperatures from room temperature to 100 K. In the case of *n*-alkane/urea inclusion compounds, the superspace group is conventionally described by using the mean structure of the host (urea) subsystem. According to our analysis of the room temperature data, the crystal is

described by the same crystallographic superspace group $P6_122(00\gamma)$ as previously determined at room temperature for other *n*-alkane/urea crystals.[20,36,38] Although the diffuse layers signify substantial displacive disorder of the guests along the ***c*** axis, in ordered regions of the crystal, the host and guest share hexagonal symmetry, and the offset between guest molecules in adjacent channels (Δ_g)[17] is zero Angstroms. The DSC traces of *n*-tetracosane/urea indicate two phase transitions from 80 K to room temperature,[37] the first at ca. 178 K, and a second, weaker one just below the first one. The first of these phase transitions presents a strong calorimetric signature, proof of a significant structural rearrangement at this temperature. This corresponds to the ferroelastic phase transition from the hexagonal superspace group to an orthorhombic one, as evidenced in the low temperature diffraction images by two different signatures. The first crystallographic signature concerns the existence of six symmetry-related orthorhombic domains.[24] This is manifested in the diffraction image shown in Figure 1d through the vertical splitting of the structure Bragg peaks. The temperature evolution of this splitting is shown in Figure 3 and leads to a transition temperature, called T_{c1}, of 179 K. The second crystallographic signature is marked by the appearance of "superstructure" Bragg peaks in the orthorhombic phase. This is clearly evidenced by comparing Figure 1c in the high symmetry phase and Figure 1d at 100 K. In Figure 1d, the superstructure Bragg peaks obey the condition $h+k$ = odd, using the orthorhombic notation (which will be designated in the following with a subscript "o").

IV. LONG-RANGE MODULATION IN THE LOWEST TEMPERATURE PHASE (PHASE III)

Because of the complexities of the phase transition at T_{c2}, it is most convenient

to first discuss the characteristics of the lowest temperature phase (Phase III). In the diffraction pattern measured at 90 K using the CRISTAL beamline at synchrotron SOLEIL, each of the superstructure lines (as denoted in Figure 1c) exhibits a set of closely-spaced Bragg peaks with maxima around 0, γ, 2γ and 1 in urea reciprocal units along $\boldsymbol{c^*}$ (Figure 4). No such closely spaced Bragg peaks appear in the structure lines (*i.e.*, with $h+k$ = even) in the orthorhombic setting. (See Figures 2b and 2c.) Very high resolution measurements are required to resolve the Bragg peaks appearing in these lines which were fit using Gaussian functions of equal widths. Essentially perfect agreement with the experimental data was obtained by fitting the superstructure Bragg peaks to multiple positions of a modulation vector $\boldsymbol{c_m^*} = (0.025 \pm 0.001)\boldsymbol{c_h^*}$, referred to common, guest, and host Bragg positions. We note that these satellite Bragg peaks vanish for values of Q just beyond γ (Figure 4a). This is interpreted as a result of the peculiar variation of the molecular form factor of the alkane guest along $\boldsymbol{c^*}$, which drops to zero just beyond $\boldsymbol{c^*} = \gamma$ (Figure 4a). (See reference 40 for details of the calculation.) This suggests that this long-range modulation is most closely associated with the guest molecules.

As stated, at 90 K, *n*-tetracosane/urea is aperiodic with $\gamma = 0.3369 \pm 0.0002$. In order to describe the new superstructure Bragg peaks, a fifth, independent reciprocal vector must be introduced. This yields the following expression for the set of vectors $\mathbf{Q}_{hklmn}$, which give the positions of the whole set of Bragg peaks in this phase:

$$\boldsymbol{Q}_{\mathbf{hklmn}} = h\,\boldsymbol{a^*} + k\,\boldsymbol{b^*} + l\,\boldsymbol{c_h^*} + m\,\boldsymbol{c_g^*} + n\,\boldsymbol{c_m^*} \qquad (2)$$

Full characterization of the diffraction pattern of this lowest temperature phase therefore requires five independent parameters (*h*, *k*, *l*, *m*, and *n*). The nomenclature concerning the first four indices *h, k*, *l* and *m* is the same as that used for the four-dimensional case discussed above. The fifth index *n* is associated with the fifth independent parameter $\boldsymbol{c_m}^*$, which appears in this orthorhombic phase and characterizes the supplementary modulation in this phase (and in Phase II). Superspace groups must be discussed in terms of the presence conditions for the (*h k l m n*) Bragg peaks (as in standard crystallography). The superspace groups of dimension five have been systematically discussed in references 42 and 43 and tabulated in reference 44. According to this work, the superspace group describing Phase III is number 19.2.18.1: $P2_12_12_1(00\gamma)(00\delta)$. The modulation vector **q** characterizing Phase III is $\boldsymbol{c_m}^* = (0,0,\delta)$, and the reflection conditions for this superspace group are 00*lmn*: *l* = even; *h*0000: *h* = even; 0*k*000: *k* = even, with no condition on the sum (*h*+*k*+*n*), as illustrated in Figure 5a. The temperature evolution of these new Bragg peaks are shown in figure 6.

As noted above, a special feature in this phase is the existence of a series of superstructure Bragg peaks, at positions $n.\delta = n.(0.025 \pm 0.001)$ in reciprocal urea units along the $\boldsymbol{c}^*$ direction. This corresponds to a long-range modulation wavelength of about 440 ± 16 Å along the channel direction. This modulation defines a very long periodicity in real space in the vicinity of 13 times the guest repeat (c_g) and 40 times the host (c_h) repeat. In the absence of a commensurate lock-in, modulation of the orientation and/or conformation of the guest component would appear to be a chemically reasonable way of generating the observed long-range modulation. This notion is supported by the intensity distribution of satellites, which coincides with the form factor of the guest molecules. However, careful fits of γ and δ in individual

frames collected on APS beamline 14-BM-C at 110 K with the detector at 980 and 440 mm do not have sufficient resolution to verify the hypothesis that the wavelength of the long-range modulation is an integral number of guest molecules.

Here, it is important to stress that the determination of a precise value of δ in phase III is very difficult since γ and δ are very close to commensurate values. At the upper end of Phase III, it is sometimes possible to observe intensity from {2 3 1 -3 0} reflections in clearly pristine regions of the crystal. Severe peak overlap makes it difficult to find an indisputable indexing of all of the additional Bragg peaks. Several measurements were performed on different crystals using different high-resolution synchrotron beamlines and, after careful fitting, yield values of δ that vary between 0.024 and 0.026.

V. A FIVE-DIMENSIONAL C-CENTERED INTERMEDIATE PHASE (PHASE II)

The temperature evolution of the superstructure lines revealed a more complex feature as the crystal was cooled through the ferroelastic phase transition (Figure 6). Using the same indexation as in Phase III, superstructure Bragg peaks with $h+k+n$ = even appeared abruptly below T_{c1}, whereas those with $h+k+n$ = odd were systematically absent upon cooling from T_{c1} to 163 K, signifying a new phase with this presence condition (Figure 6).

This intermediate phase (Phase II) also requires five dimensions to fully characterize its diffraction pattern, which exhibits additional extinction conditions. Figure 5 reveals the systematic absence of Bragg peaks ($h\ k\ l\ m\ n$) with even n in this superstructure line, in which $h+k$ = odd for any values of l and m, as shown around the

common Bragg peak (l = 0, m = 0), the alkane Bragg peak (l = 0, m = 1) and the host Bragg peak (l = 1, m = 0). In other words, the condition for the presence of the Bragg peaks in this intermediate phase is $h+k+n$ = even. In Figure 5b, which shows the temperature evolution of the averaged intensities of superstructure Bragg peaks (h k l m n), Phase III is characterized by the gradual appearance of the forbidden Bragg peaks of Phase II, *i.e.*, those with the condition $h+k+n$ odd (n = 0 in blue, n = 2 in black). The transition temperature leading from Phase II to Phase III is T_{c2} = 163 K.

In contrast with Phase III, Phase II presents the extinction conditions of a C-centered superspace group. Using the basis $\boldsymbol{a_o}^*$, $\boldsymbol{b_o}^*$, $\boldsymbol{c_h}^*$, $\boldsymbol{c_g}^*$ and $\boldsymbol{c_m}^*$, the modulation vector characterizing Phase II is $\boldsymbol{q} = (\boldsymbol{a_o}^* + \boldsymbol{c_m}^*)$, that is $\boldsymbol{q}$(1 0 0 0 1). The reflection obey the condition of $h + k + n$ = even, as shown in Figure 5b. According to reference 44, the superspace group of rank 5 that describes Phase II is number 20.2.24.2: $C222_1(00\gamma)(10\delta)$. A similar value of δ = (0.027 ± 0.001) in urea reciprocal units, is found within the limit of precision of our measurements.

This 5-D superspace group is justified even if the wavelength of this long-range modulation (approximately 408 ± 16 Å) is taken to be thirteen guest molecules because no 4-D superspace group is consistent with the observed systematic absences of $h+k+m$ = odd when γ is replaced by δ. (This condition holds near the common peak, but not in the vicinity of the first guest layer line, where odd values of n in 5-D superspace would change to even values of m in 4-D superspace, and therefore violate the absence condition.) In the high symmetry phase all channels are equivalently modulated, whereas in Phase II, there is a shift of one-half the period of the long-range modulation function in adjacent channels along the $\boldsymbol{b}$ direction. The pretransitional scattering that appears in the superstructure line when approaching the ferroelastic transition at T_{c1}

exhibits a very large correlation length along the channel axis, as extremely high-resolution studies have shown in *n*-nonadecane/urea.[41]

As revealed in Figure 7, the superstructure Bragg peaks that characterize T_{c2} exhibit a pronounced hysteresis upon warming and cooling the crystal. Indeed, both the common (n = 0, not shown) and n = 2 superstructure Bragg peaks, which characterize the low temperature phase, yield a value of T_{c2} = 175 K upon warming 163 K upon cooling.

Characterization of the modulations in Phases II and III would require crystal structure determinations in 5-D crystallographic superspace. As discussed in a previous paper,[45] the great difficulty with such a structure determination arises from the severe peak overlap due to the long-range modulation and from the six symmetry-related non-merohedral domains within the orthorhombic phase. As seen in Figure 2c, even with a synchrotron using a detector distance of 980 mm and a wavelength of 0.9787 Å, the Bragg peaks in Phase III are only just resolved along $\boldsymbol{c}^*$. Full structure determination at even modest resolution would require a detector distance of much less than 200 mm, but this would not be sufficient to resolve the peaks.

VI. CONCLUSIONS

A complex structural evolution is observed in *n*-tetracosane/urea, in some ways similar to *n*-nonadecane/urea.[36,38] However, much larger values of the modulation wavelength are observed in *n*-tetracosane/urea (λ = 408 ± 16 and 440 ± 16 Å) than in *n*-nonadecane/urea (λ = 122 Å). Surprisingly, even though both substructures are known to involve completely different interactions (hydrogen bonds for the host and van der Waals interactions for the guest), no evolution of the misfit parameter is observed as a

function of temperature. Although a significant lock-in energy was reported in another *n*-alkane/urea inclusion compound (about 3.2 kJ/mol in *n*-hexadecane/urea), no lock-in phenomenon is observed in *n*-tetracosane/urea ($\gamma = 0.3369$). Comparison with accurate guest repeats of alkane UICs determined with the mar345dtb system and with synchrotron sources indicates that c_g for *n*-tetracosane/urea is approximately 0.1 Å *shorter* than expected from other long-chain alkanes in urea. One might therefore naïvely expect that entropy of guest motion would favor selective expansion of the guest as the crystal is warmed.[17,39] However, with laboratory data obtained on the mar345dtb system (d = 150 mm), no measureable change in γ was observed between 290 and 350 K. The absence of a thermal lock-in in this system testifies to the subtle balance of host-guest interactions in alkane/urea inclusion compounds.

ACKNOWLEDGMENTS

We thank Claude Ecolivet, Tomasz Breczewski, Douglas Van Campen, Yu-Sheng Chen, Robert Henning, and Vukica Srager for their help with this work, which was supported by the PRF of the ACS (43708-AC10) and the NSF (CHE-0809845). Portions of this research were carried out at the Stanford Synchrotron Radiation Lightsource, SLAC National Accelerator Laboratory, which is supported by the U.S. Department of Energy, Office of Science, Office of Basic Energy Sciences under Contract No. DE-AC02-76SF00515 and at the Advanced Photon Source (beamline 14-BM-C) at Argonne National Laboratory, under DOE Contract No. DE-AC02-06CH11357.

References

[1] T. Janssen and A. Janner, *Acta Crystallogr. B* **70**, 617 (2014).

[2] T. Janssen, *Acta Crystallogr. A* **68**, 667 (2012).

[3] F. Axel and D. Gratias, *Beyond Quasicrystals* (Springer: Centre de Physique des Houches, 1995).

[4] A. P. Tsai, J. Q. Guo, E. Abe, H. Takakura, and T. J. Sato, *Nature* **408**, 537 (2000).

[5] R. Blinc and A. P. Levanyuk, *Incommensurate Phases in Dielectrics*, Vols. 1 and 2 (North-Holland, Amsterdam, 1986).

[6] J. M. Pérez-Mato, J. L. Ribeiro, V. Petricek, and M. I. Aroyo, *J. Phys.: Cond. Matter* **24**, 16320 (2012).

[7] M. I. McMahon, O. Degtyareva, and R. J. Nelmes, *Phys. Rev. Lett.* **85**, 4896 (2000).

[8] J. M. Hastings, J. P. Pouget, G. Shirane, A. J. Heeger, N. D Miro, and A. G. MacDiarmid, *Phys. Rev. Lett.* **39**, 1484 (1977).

[9] M. D. Hollingsworth, *Science* **295**, 2410 (2002).

[10] O. König, H.-B. Bürgi, T. Armbruster, J. Hulliger, and T. Weber, *J. Am. Chem. Soc.*, **119**, 10632 (1997).

[11] T. Janssen, A. Janner, A. Looijenga-Vos, and P. M. de Wolf, *International Tables for Crystallography*, edited by A. J. C. Wilson, Vol. C (Kluwer Academic Publishers, Dordrecht, 2006), p. 907.

[12] T. Janssen, G. Chapuis, and M. de Boissieu, *Aperiodic Crystals: From Modulated Phases to Quasicrystals* (Oxford University Press, Oxford, 2007).

[13] S. van Smaalen, *Incommensurate Crystallography* (Oxford University Press, Oxford, 2007).

[14] P. Coppens, *Acta Crystallogr. B* **51**, 402 (1995).

[15] K. D. M. Harris and J. M. Thomas, *J. Chem. Soc., Faraday Trans.* **86**, 2985 (1990).

[16] S. van Smaalen and K. D. M. Harris, *Proc. R. Soc. London*, Ser. A **452**, 677 (1996).

[17] M. D. Hollingsworth and K. D. M. Harris, in *Comprehensive Supramolecular Chemistry*, edited by D. D. MacNicol, F. Toda, and R. Bishop (Elsevier Science, Oxford, 1996), p. 177.

[18] R. Lefort, J. Etrillard, B. Toudic, F. Guillaume, T. Breczewski, and P. Bourges, *Phys. Rev. Lett.* **77**, 4027 (1996).

[19] T. Weber, H. Boysen, F. Frey, and R. B. Neder, *Acta Crystallogr. B* **53**, 544 (1997).

[20] M. Huard, B. Toudic, P. Rabiller, C. Ecolivet, L. Guérin, P. Bourges, T. Breczewski, and M. D. Hollingsworth, *J. Chem. Phys.* **136**, 104507 (2011).

[21] C. Mariette, M. Huard, P. Rabiller, S. M. Nichols, C. Ecolivet, T. Janssen, K. E. Alquist III, M. D. Hollingsworth, and B. Toudic, *J. Chem. Phys.* **136**, 104507 (2012).

[22] Y. Chatani, H. Anraku, and Y. Taki, *Mol. Cryst. Liq. Cryst.* **48**, 219 (1978).

[23] R. Forst, H. Boysen, F. Frey, H. Jagodzinski, and C. Zeyen, *J. Phys. Chem. Solids* **47**, 1089 (1986).

[24] R. Forst, H. Jagodzinski, H. Boysen, and F. Frey, *Acta Crystallogr. B* **43**, 187 (1987).

[25] R. Forst, H. Jagodzinski, H. Boysen, and F. Frey, *Acta Crystallogr. B* **46**, 70 (1990).

[26] K. Fukao, *J. Chem. Phys.* **92**, 6867 (1990).

[27] K. Fukao, T. Horiuchi, S. Taki, and K. Matsushige, *Mol. Cryst. Liq. Cryst.* **180B**, 405 (1990).

[28] K. D. M. Harris, I. Gameson, and J. M. Thomas, *J. Chem. Soc., Faraday Trans.* **86**, 3135 (1990).

[29] A. J. O. Rennie and K. D. M. Harris, *J. Chem. Phys.* **96**, 7117 (1992).

[30] R. M. Lynden-Bell, *Mol. Phys.* **79**, 313 (1993).

[31] T. R. Welberry and S. C. Mayo, *J. Appl. Crystallogr.* **29**, 353 (1996).

[32] L. Bourgeois, C. Ecolivet, B. Toudic, P. Bourges, and T. Breczewski, *Phys. Rev. Lett*. **91**, 025504 (2003).

[33] B. Toudic, F. Aubert, C. Ecolivet, P. Bourges, and T. Breczewski, *Phys. Rev. Lett.* **96**, 145503 (2006).

[34] H.-U. Lenné, H.-C. Mez, and W. Schlenk, Jr., *Justus Liebigs Ann. Chem.* **732**, 70 (1970).

[35] S. C. B. Mannsfeld, M. L. Tang, and Z. Bao, *Adv. Mater.* **23**, 127 (2011).

[36] B. Toudic, P. Garcia, C. Odin, P. Rabiller, C. Ecolivet, E. Collet, P. Bourges, G. J. McIntyre, M. D. Hollingsworth, and T. Breczewski, *Science* **319**, 69 (2008).

[37] T. Breczewski, private communication.

[38] B. Toudic, P. Rabiller, L. Bourgeois, M. Huard, C. Ecolivet, G. J. McIntyre, P. Bourges, T. Breczewski, and T. Janssen, *Europhys. Lett.* **93**, 16003 (2011).

[39] M. D. Hollingsworth, K. D. M. Harris, W. Jones, and J. M. Thomas, *J. Inclus. Phenom.* **5**, 273 (1987).

[40] P. Rabiller, J. Etrillard, L. Toupet, J. M. Kiat, P. Launois, V. Petricek, and T. Breczewski, *J. Phys.: Cond. Matter* **13**, 1653 (2001)

[41] C. Mariette, L. Guérin, P. Rabiller, C. Ecolivet, P. García-Orduña, P. Bourges, A. Bosak, D. de Sanctis, M. D. Hollingsworth, T. Janssen, and B. Toudic, *Phys. Rev. B* **87**, 104101 (2013)

[42] H. T. Stokes, B. J. Campbell, and S. van Smaalen, *Acta Crystallogr. A*, **67**, 45 (2011).

[43] S. van Smaalen, B. J. Campbell, and H. T. Stokes, *Acta Crystallogr. A*, **69**, 75(2013).

[44] ISOTROPY Software Suite, iso.byu.edu.

[45] C. Mariette, L. Guérin, P. Rabiller, Y.-S. Chen, A. Bosak, A. Popov, M. D. Hollingsworth, and B. Toudic, *Z. Kristallogr*., **230**, 5 (2015).

Figure 1

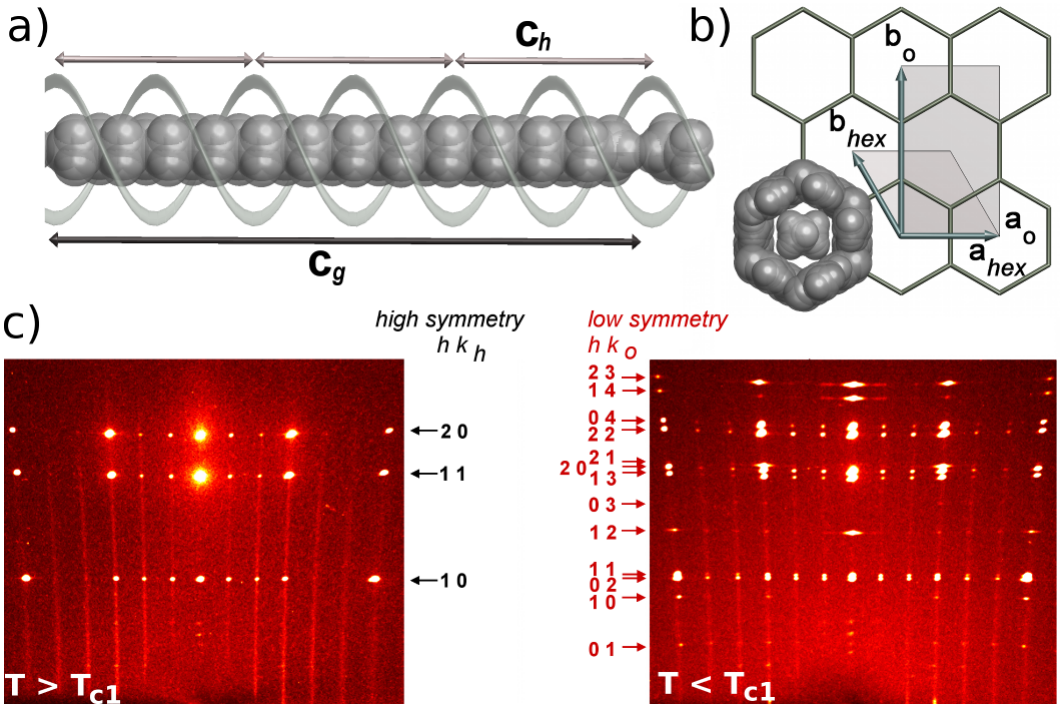

FIG. 1. a) *n*-Tetracosane/urea viewed perpendicular to the channel axis with the host shown schematically; b) projection of the *n*-tetracosane/urea structure onto the ***ab*** plane (with arbitrary guest orientation) showing the hexagonal and orthorhombic definitions of the basis vectors. Throughout this paper, Miller planes indexed with these cells are denoted with subscripts "h" and "o". c) 60° rotating crystal X-ray diffraction images, obtained on the mar345dtb system using Cu-K_α radiation and measured in the high-symmetry phase (Phase I) at room temperature (left) and in the lowest symmetry phase (Phase III) at 100 K (right). The guest diffraction appears as diffuse layers perpendicular to ***c**** (which is horizontal) with superimposed Bragg peaks. Miller indices (*h k*) along the reciprocal directions ***a**** and ***b**** correspond to the hexagonal cell for the HS phase and the orthorhombic cell for Phase III (and Phase II, which is not shown).

Figure 2

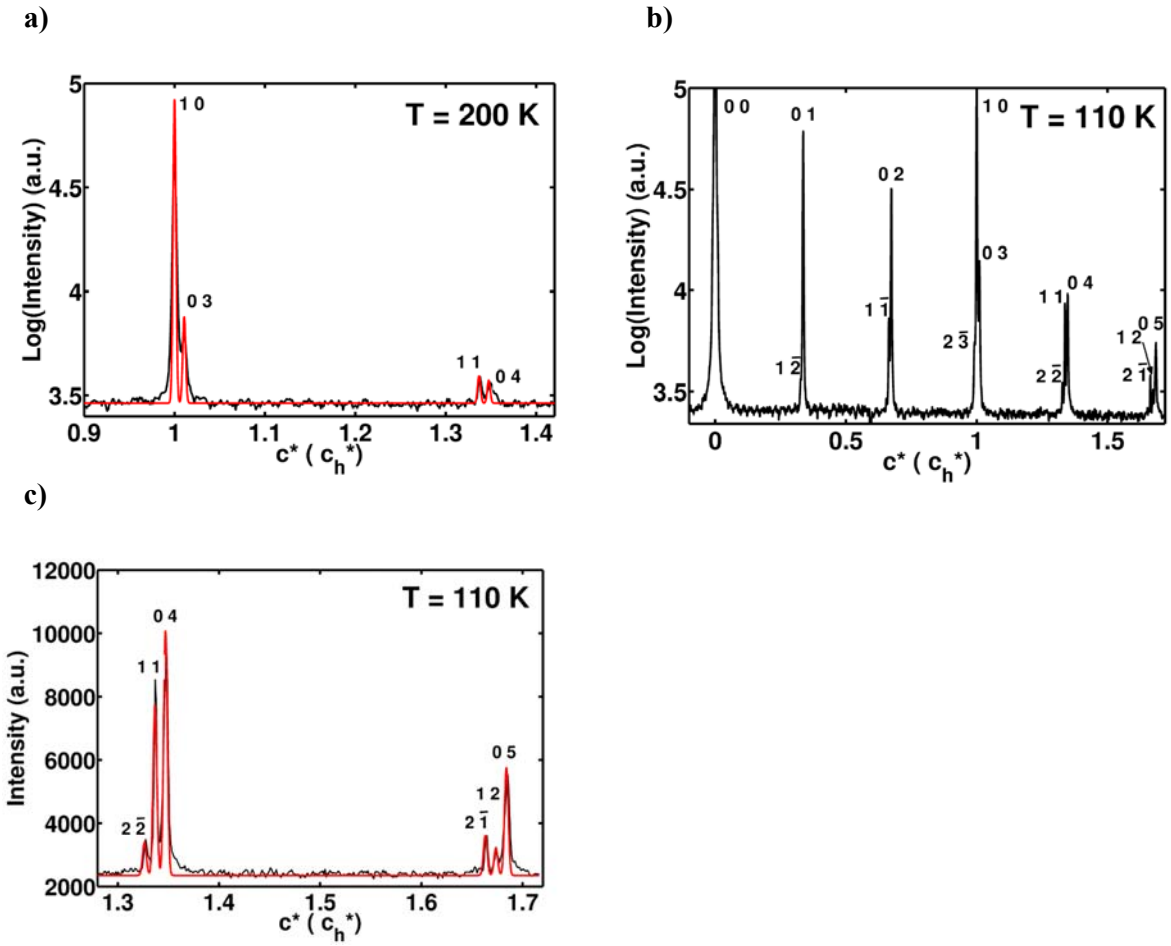

FIG. 2. Profiles along c^* using a detector distance of 980 mm on beamline 14-BM-C at the APS. a) Profile (logarithmic intensity scale) and fit of a section of the $(1\ 0\ l\ m)_h$ layer line of Phase I at 200 K with $\gamma = 0.3369 \pm 0.0005$. The l and m indices are shown next to each Bragg peak. b) Profile (logarithmic intensity scale) of the equivalent $(0\ 2\ l\ m\ n)_o$ layer line of Phase III at 110 K showing the values of l and m for each assigned peak. (In this structure line, $n = 0$ in all cases.) c) An enlargement of the profile of the $(0\ 2\ l\ m\ n)_o$ layer line of Phase III at 110 K from Q(c_h^*) of 1.3 to 1.7 (linear intensity scale) showing the l and m indices and the corresponding fit with $\gamma = 0.3369 \pm 0.0002$. In these structure lines at 200 and 110 K, all of the Bragg peaks can be fit with Gaussian functions at the combinatory positions for l and m.

Figure 3

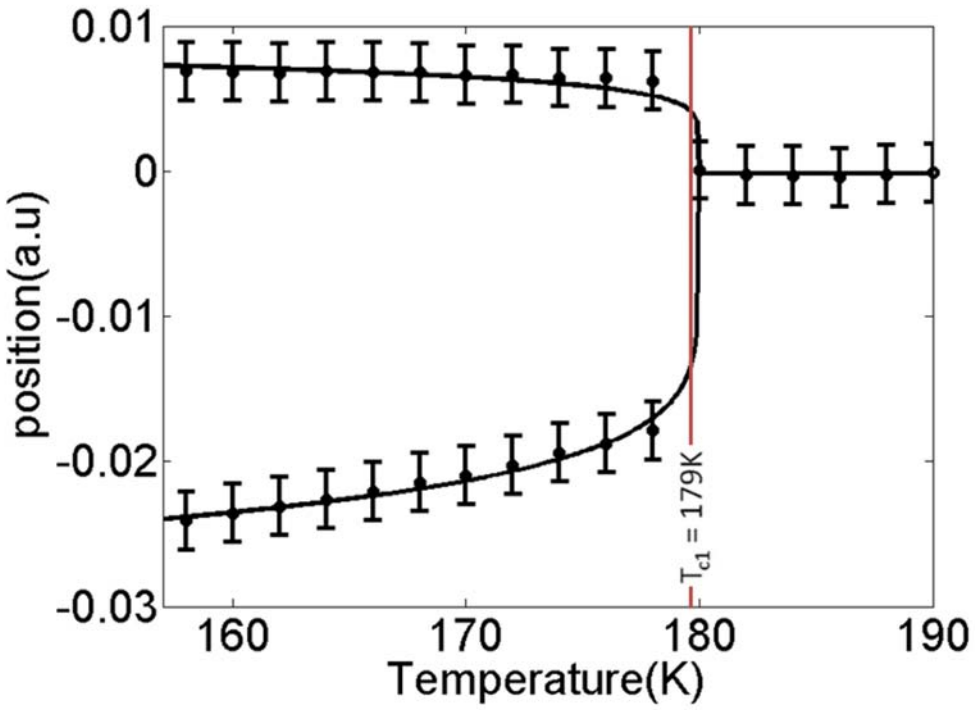

FIG. 3. Evidence for the ferroelastic phase transition from hexagonal to orthorhombic symmetry at T_{c1} = 179 K in *n*-tetracosane/urea, through the domain-induced splitting of a structure Bragg peak. Here the $(20l)_h$ structure line splits into the $(22l)_o$ and $(04l)_o$ structure lines (*cf*. Figure 1c).

Figure 4

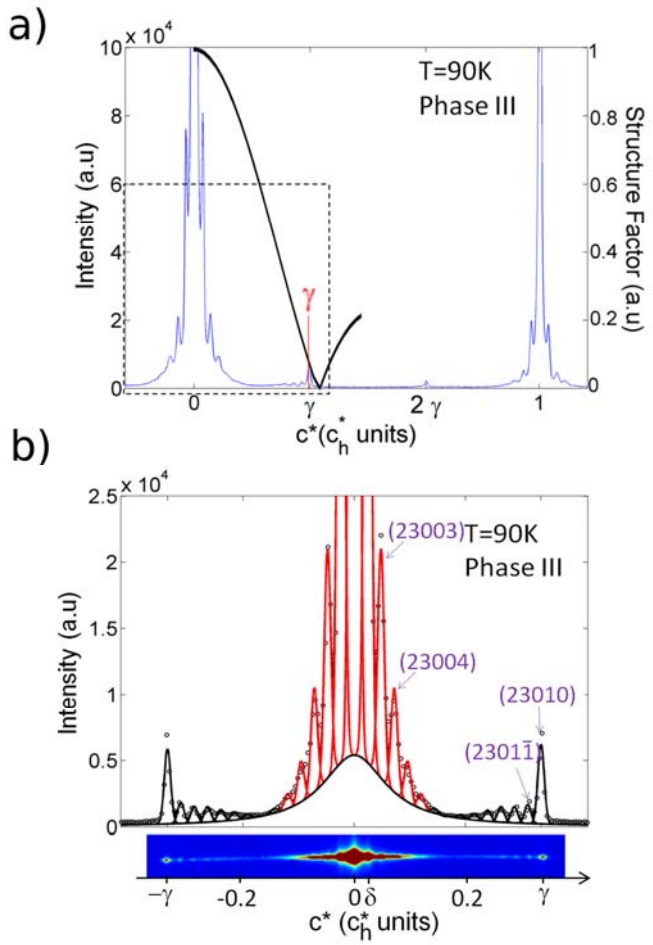

FIG. 4. a) *n*-Tetracosane/urea (2 3 0 *m n*)$_o$ superstructure line (in blue) measured at 90 K on the CRISTAL beamline at SOLEIL along the incommensurate direction in the $\boldsymbol{q}$ range of -0.2$\boldsymbol{c_h}$* to 1.2$\boldsymbol{c_h}$* in reciprocal urea units; Inset in black: Molecular form factor of the *n*-tetracosane molecule aligned along the $\boldsymbol{c}$ direction with six-fold orientational disorder, as calculated in [40]. b) Diffraction image and extracted profile of the (2 3 0 *m n*)$_o$ superstructure line between -0.4$\boldsymbol{c_h}$* and +0.4$\boldsymbol{c_h}$*. Superstructure satellite Bragg peaks are associated with a modulation vector $\boldsymbol{c_m}$* = ± (0.025 ± 0.001)$\boldsymbol{c_h}$*. Satellite peaks were fit using Gaussians and are indexed as (2 3 0 0 *m*)$_o$ in red and (2 3 0 1 *m*)$_o$ in black.

Figure 5

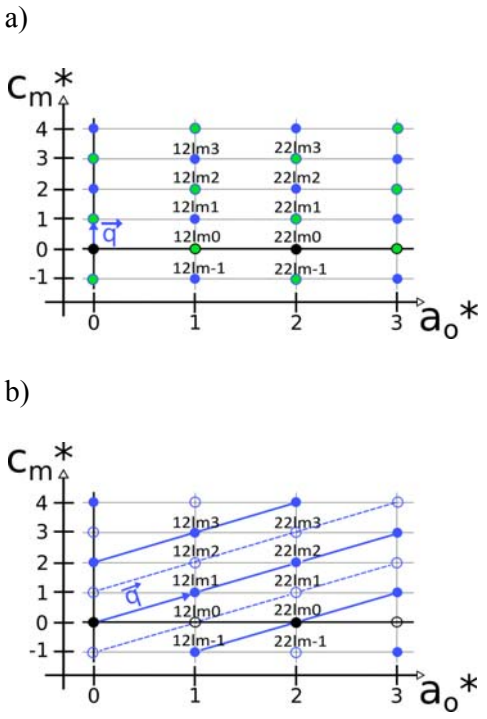

FIG. 5. a) Schematic representation of the (a_o*,c*) diffraction plane for k = 2 in phase III of *n*-tetracosane/urea: the black points denote the structure Bragg peaks of the high symmetry phase, whereas the blue and green points indicate the positions of Bragg peaks representing the supplementary modulation; b) schematic representation of the same diffraction plane in Phase II: black points refer to structure Bragg peaks of the high symmetry phase, blue points indicate the positions of Bragg peaks that appear in Phase II. Open circles indicate the Bragg peaks that are missing in Phase II, but present in Phase III (and shown in green in Figure 5a).

Figure 6

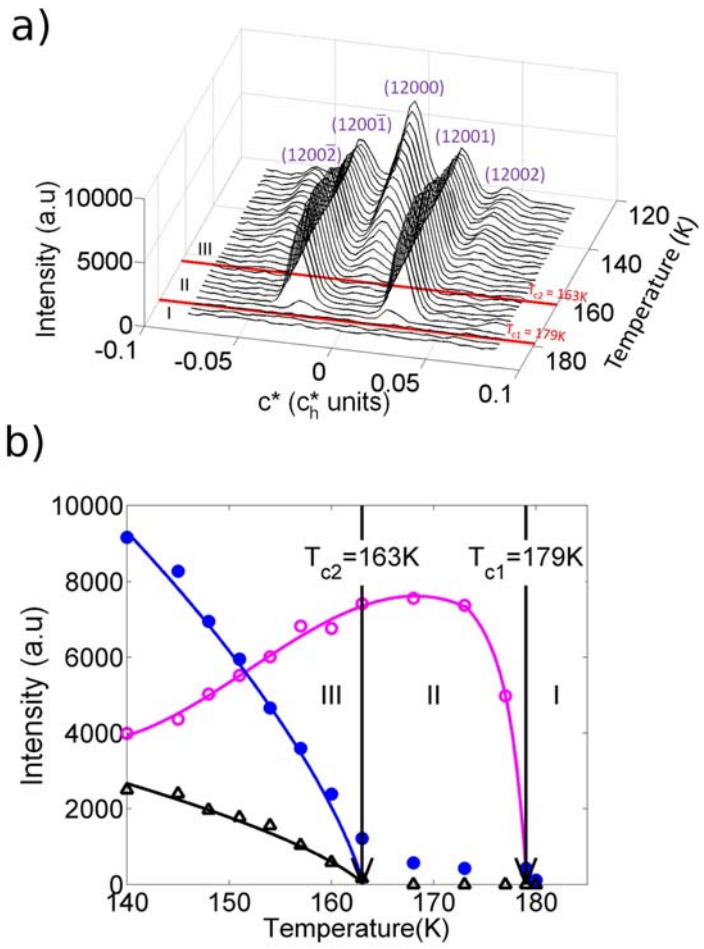

FIG. 6. a) Temperature evolution of the superstructure line (h = 1, k = 2) measured on the mar345dtb system using Cu-K_α radiation revealing two phase transitions at T_{c1} = 179 K and T_{c2} = 163 K. b) Extracted temperature evolution of the averaged intensities of superstructure Bragg peaks (h k l m n), which demonstrate that h+k+n = odd Bragg peaks characterize Phase III (n = 0 in blue filled circles, n = 2 in black triangles) and that h+k+n = even Bragg peaks characterize Phase II (n = 1 in pink circles).

Figure 7 :

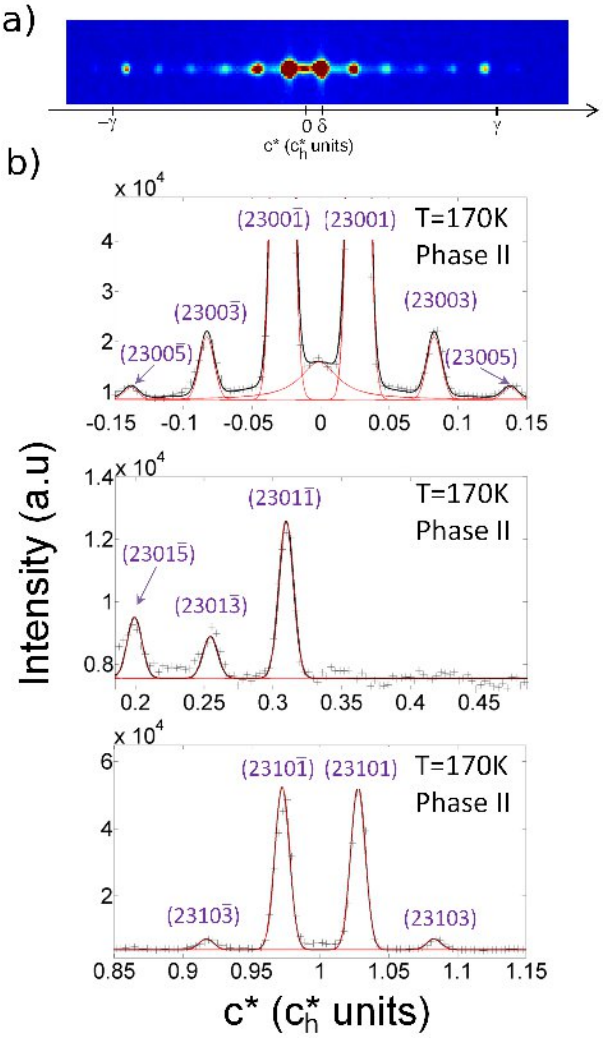

FIG. 7. a) High-resolution diffraction image of the superstructure line (h = 2, k = 3) measured at SSRL (T = 170 K). b) Evidence of an intermediate phase characterized by the presence of Bragg peaks with h+k+n = even, as shown here in the (2 3 l m n) superstructure line with h+k = 5. The profiles were measured around the common (l = m = 0) position (top), around the guest (l = 0, m = 1) position (middle), and host (l = 1, m = 0) position (bottom).

Figure 8

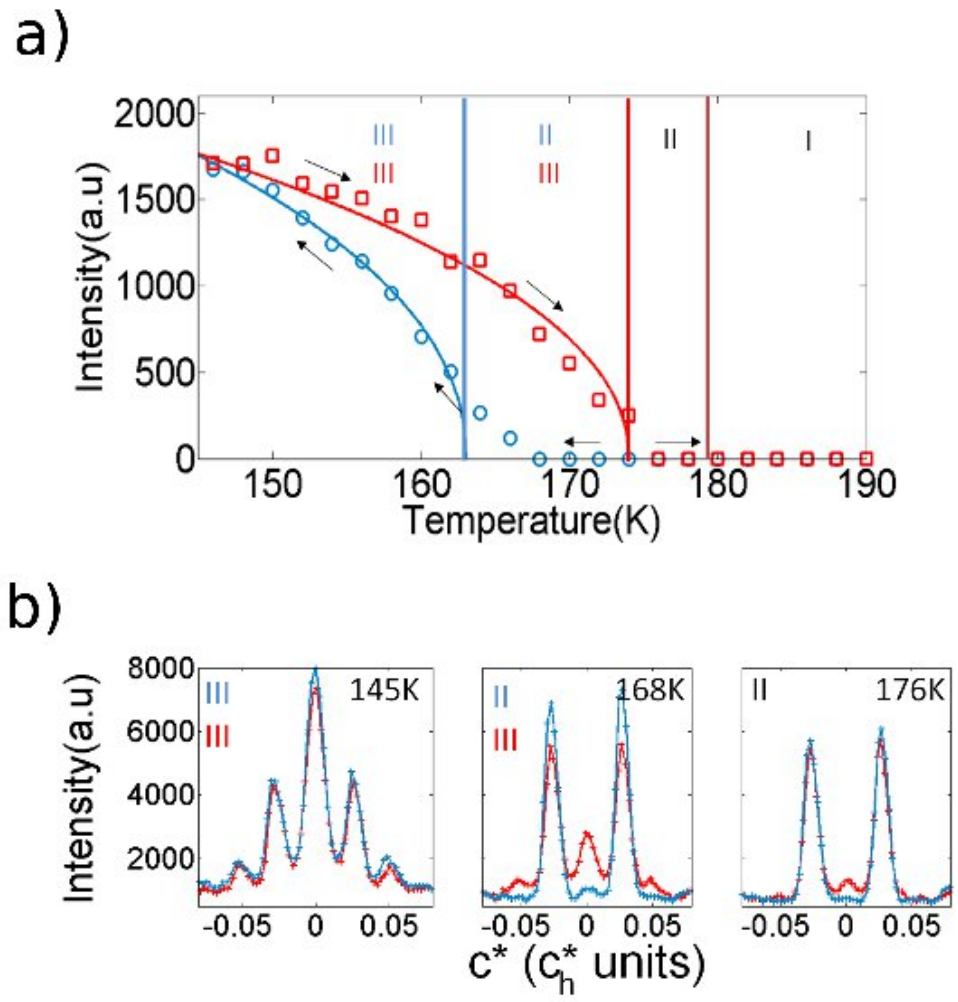

FIG. 8. a) Temperature evolution of the intensity of the superstructure Bragg peaks verifying h=1 and k=2 of order n = 2, when increasing (red squares) and decreasing (blue circles) the temperature. b) The n = 2 satellite Bragg peak is absent at 176 K and present at 145 K. At 168 K, it is present upon warming (in red) and absent upon cooling (in blue), revealing the hysteresis behavior of the second phase transition.